Journal of Intensive Care Medicine
2021, Vol. 36(8) 900-909

DOI: 10.1177/08850666211006335
journals.sagepub.com/home/jic


Right Ventricular Strain Is Common in Intubated COVID-19 Patients and Does Not Reflect Severity of Respiratory Illness

Lauren E. Gibson, MD[1], Raffaele Di Fenza, MD[1], Min Lang, MD, MSc[2], Martin I. Capriles[1], Matthew D. Li, MD[2], Jayashree Kalpathy-Cramer, PhD[2], Brent P. Little, MD[2], Pankaj Arora, MD[3], Ariel L. Mueller, MA[1], Fumito Ichinose, MD, PhD[1], Edward A. Bittner, MD, PhD[1], Lorenzo Berra, MD[1], and Marvin G. Chang, MD, PhD[1]; for the Nitric Oxide Study Investigators

Abstract

Background: Right ventricular (RV) dysfunction is common and associated with worse outcomes in patients with coronavirus disease 2019 (COVID-19). In non-COVID-19 acute respiratory distress syndrome, RV dysfunction develops due to pulmonary hypoxic vasoconstriction, inflammation, and alveolar overdistension or atelectasis. Although similar pathogenic mechanisms may induce RV dysfunction in COVID-19, other COVID-19-specific pathology, such as pulmonary endothelialitis, thrombosis, or myocarditis, may also affect RV function. We quantified RV dysfunction by echocardiographic strain analysis and investigated its correlation with disease severity, ventilatory parameters, biomarkers, and imaging findings in critically ill COVID-19 patients. **Methods:** We determined RV free wall longitudinal strain (FWLS) in 32 patients receiving mechanical ventilation for COVID-19-associated respiratory failure. Demographics, comorbid conditions, ventilatory parameters, medications, and laboratory findings were extracted from the medical record. Chest imaging was assessed to determine the severity of lung disease and the presence of pulmonary embolism. **Results:** Abnormal FWLS was present in 66% of mechanically ventilated COVID-19 patients and was associated with higher lung compliance (39.6 vs 29.4 mL/cmH_2O, $P = 0.016$), lower airway plateau pressures (21 vs 24 cmH_2O, $P = 0.043$), lower tidal volume ventilation (5.74 vs 6.17 cc/kg, $P = 0.031$), and reduced left ventricular function. FWLS correlated negatively with age ($r = -0.414$, $P = 0.018$) and with serum troponin ($r = 0.402$, $P = 0.034$). Patients with abnormal RV strain did not exhibit decreased oxygenation or increased disease severity based on inflammatory markers, vasopressor requirements, or chest imaging findings. **Conclusions:** RV dysfunction is common among critically ill COVID-19 patients and is not related to abnormal lung mechanics or ventilatory pressures. Instead, patients with abnormal FWLS had more favorable lung compliance. RV dysfunction may be secondary to diffuse intravascular micro- and macro-thrombosis or direct myocardial damage. **Trial Registration:** National Institutes of Health #NCT04306393. Registered 10 March 2020, https://clinicaltrials.gov/ct2/show/NCT04306393

Keywords

COVID-19, acute respiratory distress syndrome, right ventricle, strain, cardiac dysfunction

Introduction

Among patients hospitalized with coronavirus disease 2019 (COVID-19), an estimated 20% to 25% will exhibit cardiac involvement which has been associated with worse outcomes.[1,2] Right ventricular (RV) dysfunction is the most common cardiac abnormality and has been noted in between 30% and 40% of hospitalized patients across varying disease severity.[3,4]

Whether intubated patients with COVID-19 are more prone to developing RV dysfunction than non-COVID-19 populations with acute respiratory distress syndrome (ARDS) remains

[1] Department of Anesthesia, Critical Care, and Pain Medicine, Massachusetts General Hospital, Boston, MA, USA
[2] Department of Radiology, Massachusetts General Hospital, Boston, MA, USA
[3] Division of Cardiovascular Disease, University of Alabama at Birmingham, Birmingham, AL, USA

Received March 02, 2021. Received revised March 02, 2021. Accepted March 11, 2021.

Corresponding Author:
Marvin G. Chang, Massachusetts General Hospital, 55 Fruit Street, GRB 444, Boston, MA 02114, USA.
Email: mgchang@mgh.harvard.edu

unknown. In non-COVID ARDS, RV dysfunction has been attributed to the sustained elevation in pulmonary vascular resistance resulting from pulmonary hypoxic vasoconstriction, inflammatory infiltrates, and alveolar overdistension and atelectasis during positive pressure ventilation.[5,6] Impaired microperfusion and direct inflammatory injury leading to myocardial contractile dysfunction may also play a role.[7,8] To what extent the development of RV dysfunction in COVID-19 infection can be attributed to these factors versus COVID-19-specific pathology, such as endothelialitis or viral myocarditis is unclear.[9,10] Recent autopsy studies and radiographic findings have identified abnormalities of pulmonary vasculature as distinguishing feature of COVID-19 illness, including endothelial destruction, widespread thrombosis, abnormal vessel dilation, and angiogenesis.[9-12] We hypothesize that RV dysfunction in COVID-19 is different from that in non-COVID ARDS due to a greater degree of pulmonary vascular dysfunction rather than alveolar damage.

While standard echocardiography remains a valuable tool for evaluation of RV function and estimation of pulmonary pressures, speckle-tracking echocardiography has emerged as a promising technique for detecting subclinical cardiac impairment that may have prognostic implications.[13(p20)] RV free wall longitudinal strain (FWLS) assessed by speckle-tracking echocardiography has been shown to correlate with outcomes in a variety of disease processes, including most recently as a predictor of mortality in COVID-19.[14] In order to explore the characteristics of RV dysfunction in severe COVID-19 infection, we quantified FWLS and investigated its correlation with disease severity, ventilatory parameters, inflammatory markers, and chest imaging findings in a cohort of critically ill patients receiving mechanical ventilation.

Methods

This study was approved by the Mass General Brigham Institutional Review Board (2020P000787) and informed consent was obtained from each patient or their surrogate prior to enrollment. Subjects in this study were enrolled as part of a larger randomized controlled trial of nitric oxide for the treatment of COVID-19 which has been described elsewhere.[15] In this ancillary study, we performed transthoracic echocardiography in 32 patients within 72 hours of admission to an intensive care unit with COVID-19 respiratory failure and prior to administration of inhaled nitric oxide. All patients were receiving mechanical ventilation at the time of exam.

Demographic data, comorbid conditions, ventilatory parameters, medications, and inflammatory markers were extracted from the electronic medical record. Ventilatory parameters included airway plateau pressure, tidal volume, positive end expiratory pressure (PEEP), fraction of inspired oxygen, pH, and arterial partial pressures of oxygen and carbon dioxide. Lung compliance was calculated as the tidal volume divided by the difference between plateau pressure and PEEP. The P/F ratio was calculated as the arterial partial pressure of oxygen divided by the fraction of inspired oxygen. Recorded laboratory findings included high-sensitivity troponin, platelet count, D-dimer, ferritin, lactate dehydrogenase, creatinine kinase, C-reactive protein, and serum creatinine. Laboratory data were taken from the time of admission to the intensive care unit. The acute physiologic assessment and chronic health evaluation II (APACHE II) score[16] and sequential organ failure assessment (SOFA) score[17] were calculated for each patient as indicators of clinical disease severity. The vasoactive-inotropic score (VIS)[18] was calculated from the doses of vasopressors and/or inotropes each patient was receiving at the time of echocardiographic examination. The presence of acute kidney injury (AKI) was determined based on an elevation in serum creatinine by at least 0.3 mg/dL from the patient's prior baseline or, if no baseline was available, from the time of hospital presentation.

Echocardiographic Assessment

Echocardiographic images were obtained using a Philips CX50 (Andover, MA) portable ultrasound machine with a phased array transducer. Studies were interpreted by an intensivist certified in critical care echocardiography by the National Board of Echocardiography. RV assessments included chamber size, tricuspid annular plane systolic excursion (TAPSE), and peak systolic tricuspid annular velocity (S') by tissue Doppler imaging. Right ventricular systolic pressure (RVSP) was estimated as the sum of the peak gradient from the tricuspid regurgitation jet and central venous pressure (CVP) measured from a central venous catheter. In patients without CVP transduction from a central venous catheter, CVP was approximated based on IVC size and collapsibility. A CVP of 5 mmHg was used if the IVC was < 2.1 cm and collapsible, and a CVP of 10 mmHg was used if the IVC was > 2.1 cm and plethoric.[19] An RVSP greater than 35 mmHg was considered elevated. RV dilation was determined based on a basal diameter of 4.2 cm or greater and RV systolic dysfunction was determined based on TAPSE less than 1.8 cm, as this cutoff was previously shown to best predict survival in patients with pulmonary hypertension.[20] LV assessments included mitral inflow signal (E and A) by spectral Doppler, diastolic velocities of the lateral mitral annulus (e' and a') by tissue Doppler, and the LV outflow tract velocity time integral, which was used as a correlate for cardiac output. Left atrial pressure was estimated from the ratio of E/e' and values greater than 14 mmHg were considered elevated.[21]

Strain Analysis

In addition to the echocardiographic parameters described above, we determined RV free wall longitudinal strain (FWLS) by 2D speckle-tracking imaging. Strain was calculated for all patients using EchoInsight (Epsilon Imaging, Ann Arbor, Michigan) software. An automated tracing of the RV endocardial border was generated from the apical 4-chamber view, and manual corrections were performed to encompass the RV wall thickness. End-diastole was identified as the frame occurring at

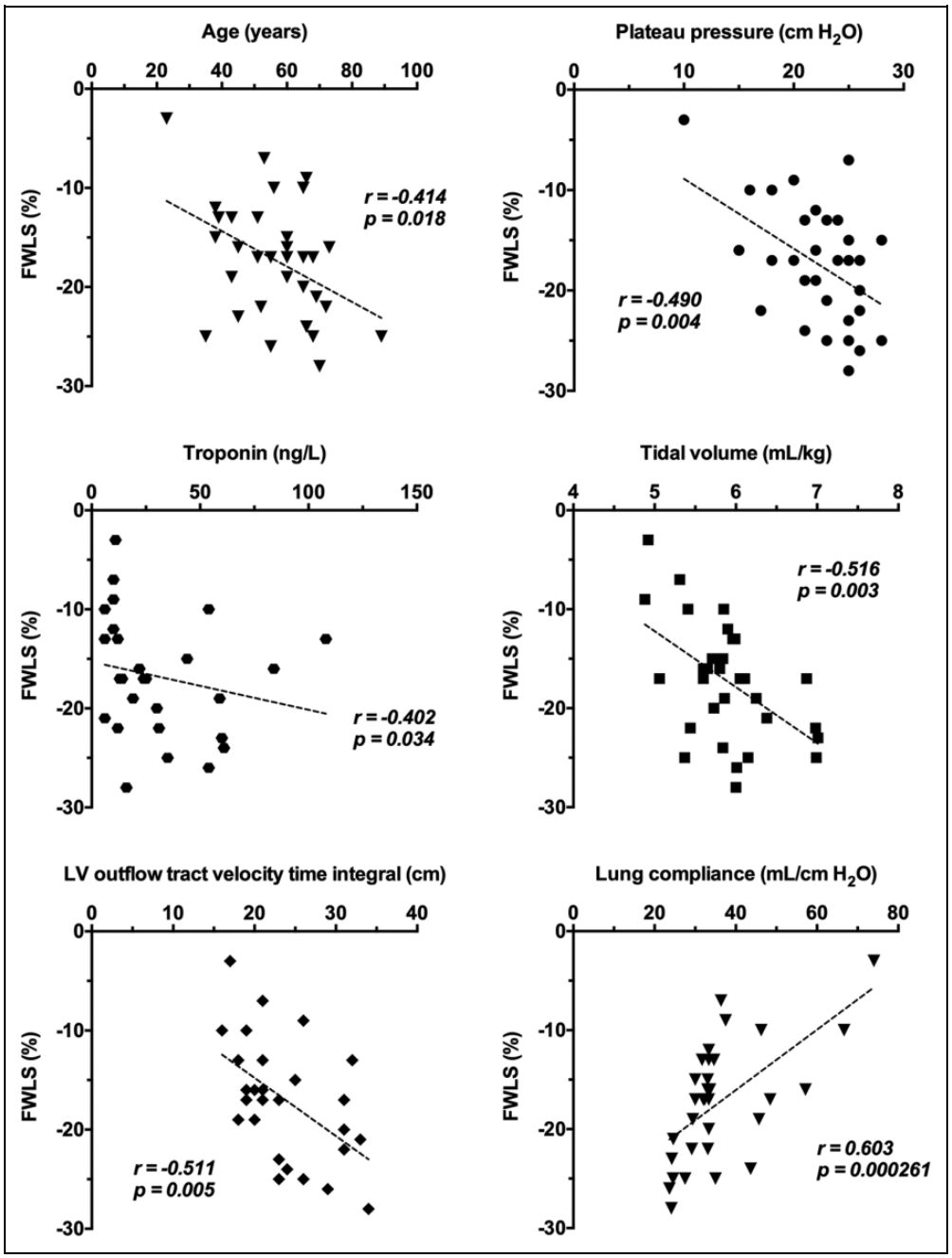

Figure 1. Correlations between right ventricular free wall longitudinal strain (FWLS) and patient characteristics. FWLS negatively correlated with age (A), high-sensitivity troponin level at the time of ICU admission (B) and left ventricular (LV) outflow tract velocity time integral (C), a marker for cardiac stroke volume. In terms of respiratory parameters, FWLS negatively correlated with (D) airway plateau pressure and (E) tidal volume, while FWLS positively correlated with (F) lung compliance.

the peak of the QRS complex, while end-systole was identified as the frame in which the RV cavity was the smallest. The RV endocardial border was then automatically tracked throughout the cardiac cycle. The initial region of interest included both the RV free wall and septum (Supplemental Figure 1) and in accordance with recent guidelines,[22] FWLS was automatically calculated as the mean of the basal, mid, and apical strain values of the RV free wall after excluding the septal strain values. Longitudinal strain, representing the percent change in length of a myocardial segment during systole, is expressed as a negative value due to fiber shortening. FWLS greater than -20% was considered abnormal based on published reference ranges.[23]

Chest Imaging Findings

Portable chest radiographs obtained within 24 hours of endotracheal intubation were assessed using a previously validated

Table 1. Demographics of Intubated COVID-19 Patients.

	All (n = 32)	Normal FWLS (n = 11)	Abnormal FWLS (n = 21)	*P* value
Age, mean ± SD	56 ± 14	62 ± 15	53 ± 13	0.066
Male sex, n (%)	21 (66%)	4 (36%)	17 (81%)	0.011
BMI (kg/m^2), median (IQR)	30.4 (26.6−34.5)	31.5 (27.4−33.6)	29.5 (25.7−34.8)	0.725
Hx of HTN, n (%)	16 (50%)	6 (55%)	10 (48%)	0.721
Hx of diabetes, n (%)	13 (41%)	3 (27%)	10 (48%)	0.280
Hx of CKD, n (%)	9 (28%)	4 (36%)	5 (24%)	0.469
Hx of tobacco use, n (%)	12 (38%)	5 (45%)	7 (33%)	0.517
Hx of malignancy, n (%)	9 (28%)	5 (45%)	4 (19%)	0.122

Abbreviations: FWLS, free wall longitudinal strain; SD, standard deviation; IQR, interquartile range; BMI, body mass index, HTN, hypertension; CKD, chronic kidney disease.

convolutional Siamese neural network-based approach for automated assessment of COVID-19 lung disease severity, called the pulmonary x-ray severity (PXS) score.[24,25] In brief, this machine learning model takes pixel-level image data from frontal chest radiographs as inputs and outputs a quantitative score for consolidative lung disease severity, which has been shown to correlate with manual assessment of COVID-19 radiographic disease severity by multiple radiologists. In this scheme, a PXS score ≤ 2.5 indicates normal/minimal disease, > 2.5 and ≤ 5.0 mild disease, > 5.0 and ≤ 9.0 moderate disease, and > 9.0 severe disease. DICOM files for the chest radiographs of interest were exported from our institution's picture archiving and communication system and processed using the PXS score algorithm. Fifteen patients underwent CT pulmonary angiography and were assessed by a thoracic radiologist for presence of pulmonary emboli (PE).

Statistical Methods

Normally distributed data are presented as mean ± standard deviation and compared using the independent samples t-test. Nonnormally distributed data are presented by the median and first and third quartiles and compared using the Wilcoxon rank-sum test. Normality was determined with the Shapiro-Wilk test. Correlation between FWLS and continuous variables was determined by Pearson (normally distributed variables) or by Spearman (nonnormally distributed variables) correlation. $P < 0.05$ was considered to indicate statistical significance. Data were analyzed using SPSS version 24 (IBM Corp., Armonk, NY).

Results

Demographics

Among the 32 patients studied, 66% (n = 21) were male and the average age was 56 ± 14 years. Six patients (19%) had major pre-existing cardiac disease, including severe mitral regurgitation (n = 1), left ventricular (LV) hypertrophy (n = 3), and ischemic cardiomyopathy (n = 2). None of the patients had pre-existing pulmonary hypertension or RV dysfunction prior to admission for COVID-19 infection. Abnormal FWLS was present in 21 of 32 patients (66%). Abnormal strain was associated with male gender ($P = 0.011$) and FWLS was negatively correlated with age ($r = -0.414$, $P = 0.018$; Figure 1). There was no association between abnormal strain and BMI or medical co-morbidities (Table 1).

Clinical Risk Scores and Laboratory Findings

Patients with abnormal and normal FWLS had similar disease severity by the APACHE and SOFA scores, similar vasopressor and inotrope requirements by the VIS (4.7 vs 6.2, $P = 0.725$), and similar rates of AKI (48% vs 64%, $P = 0.405$). In terms of laboratory findings, abnormal FWLS was associated with a lower platelet count (218 vs 317 $10^3/\mu L$, $P = 0.016$) and a trend toward higher ferritin levels (1697 vs 963 ug/L, $P = 0.123$). FWLS was negatively correlated with high-sensitivity troponin level ($r = -0.402$, $P = 0.034$; Figure 1). There were no other differences in inflammatory markers between patients with and without abnormal strain patterns (Table 2) and no other correlations between FWLS and laboratory findings (Supplemental Table 1).

Respiratory Parameters

Patients with abnormal FWLS were receiving lower tidal volume ventilation (5.74 vs 6.17 cc/kg, $P = 0.031$), lower airway plateau pressures (21 vs 24 cm H_2O, $P = 0.043$), and had higher lung compliance (39.6 vs 29.4 mL/cm H_2O, $P = 0.016$) than those with normal RV function. Patients with abnormal FWLS also trended toward lower positive end expiratory pressures (11 vs 13 cm H_2O; $P = 0.153$). FWLS negatively correlated with tidal volume ($r = -0.516$, $P = 0.003$) and airway plateau pressure ($r = -0.490$, $P = 0.004$), and positively correlated with lung compliance ($r = 0.602$, $P = 0.006$; Figure 1). There were no differences in pH, carbon dioxide levels, or oxygenation between patients with normal and abnormal FWLS (Table 3).

Echocardiographic Data

Five patients (16%), all with abnormal FWLS, had evidence of RV systolic dysfunction by TAPSE. Thirteen of our

Table 2. Clinical Risk Scores and Laboratory Findings Among COVID-19 Patients.

	All (n = 32)	Normal FWLS (n = 11)	Abnormal FWLS (n = 21)	*P* value
APACHE score, median (IQR)	23 (19-26)	26 (21-26)	23 (18-25)	0.180
SOFA score, mean ± SD	8.4 ± 2.4	8.1 ± 2.2	8.5 ± 2.5	0.627
VIS, median (IQR)	4.9 (0-12.2)	6.2 (1.39-13.8)	4.7 (0-10.5)	0.725
HS troponin (ng/L), median (IQR)	22 (11-52)	31 (16-54)	19 (11-35)	0.656
Elevated HS troponin*, n (%)	19 (59%)	8 (73%)	11 (52%)	0.108
Platelet count (k/uL), mean ± SD	252 ± 113	317 ± 103	218 ± 105	0.016
D-dimer (ng/mL), median (IQR)	2118 (1324-3732)	2032 (1110–3016)	2203 (1351–4184)	0.457
Ferritin (ug/L), median (IQR)	1439 (843-2811)	963 (386-1262)	1697 (981-3013)	0.123
LDH (U/L), median (IQR)	441 (337-647)	524 (439-667)	398 (319-625)	0.144
CK (U/L), median (IQR)	198 (78-937)	111 (59-383)	454 (81-1022)	0.261
CRP (mg/L), median (IQR)	146 (118-229)	143 (103-225)	146 (134-210)	0.855
AKI, n (%)	18 (56%)	7 (64%)	11 (48%)	0.405

Abbreviations: FWLS, free wall longitudinal strain; SD, standard deviation; IQR, interquartile range; APACHE, acute physiologic assessment and chronic health evaluation II; SOFA, sequential organ failure assessment; VIS, vasoactive inotropic score; HS, high-sensitivity; LDH, lactate dehydrogenase; CK, creatinine kinase; CRP, C-reactive protein; AKI, acute kidney injury.
*HS troponin was considered elevated if >15 ng/L (men) or >10 ng/L (women).

Table 3. Respiratory Parameters Among Intubated COVID-19 Patients.

	All (n = 32)	Normal FWLS (n = 11)	Abnormal FWLS (n = 21)	*P* value
PEEP (cm H_2O), mean ± SD	11 ± 3.4	13 ± 3.1	11 ± 3.5	0.153
Plateau P (cm H_2O), mean ± SD	22 ± 4.2	24 ± 3.0	21 ± 4.4	0.043
TV (cc/kg), mean ± SD	5.89 ± 0.54	6.17 ± 0.60	5.74 ± 0.46	0.031
Lung compliance (mL/cm H_2O), median (IQR)	33.2 (29.9-36.9)	27.5 (24.4-33.2)	33.3 (32.3-45.7)	0.004
FiO_2, median (IQR)	50% (40%-60%)	50% (40%-70%)	50% (40%-60%)	0.457
pH, mean ± SD	7.36 ± 0.08	7.38 ± 0.09	7.35 ± 0.07	0.256
PaO_2 (mm Hg), median (IQR)	87 (79-119)	90 (82-121)	87 (79-118)	0.938
$PaCO_2$ (mm Hg), mean ± SD	46 ± 9.0	44 ± 6.3	46 ± 10	0.463
P/F ratio, median (IQR)	179 (147-224)	180 (171-201)	178 (137-258)	0.785

Abbreviations: FWLS, free wall longitudinal strain; SD, standard deviation; IQR, interquartile range; PEEP, positive end expiratory pressure; P, pressure; TV, tidal volume; FiO_2, fraction of inspired oxygen; P/F ratio, PaO_2/FiO_2.

patients (42%) met criteria for pulmonary hypertension (RVSP > 35 mmHg) and 14 patients (44%) had evidence of RV dilation. Neither pulmonary hypertension nor RV dilation were associated with abnormal strain (Table 4), nor did FWLS correlate with RVSP or RV basal diameter (Supplemental Table 1). LV dysfunction was overall uncommon in our population. Four patients (13%) had elevated left atrial pressures and 2 patients (7.1%) had a reduced LV outflow tract velocity time integral (< 18 cm). Abnormal RV FWLS was associated with reduced LV stroke volume based the LV outflow tract velocity time integral (21.7 vs 28.1 cm, $P = 0.001$) as well as reduced late diastolic mitral annular velocity (a') by tissue Doppler (11.6 vs 14.6 cm/s, $P = 0.026$). There was also a trend of lower late diastolic filling velocity (A) by spectral Doppler in patients with abnormal FWLS (71.4 vs 87.1 cm/s, $P = 0.053$). FWLS also correlated with both LV outflow tract velocity time integral ($r = -0.511$, $P = 0.005$; Figure 1) and late diastolic mitral annular velocity (a') ($r = -0.383$, $P = 0.037$; Supplemental Table 1).

Imaging Findings

Post-intubation chest radiographs were available for 31 out of 32 patients. Images were not available for 1 patient who was transferred from an outside facility. There was no difference in severity of pulmonary disease between patients with and without abnormal FWLS as assessed by the PXS score, a deep learning-based automated radiographic score for COVID-19 lung disease severity (8.24 ± 2.70 vs 9.33 ± 1.56, $P = 0.205$) (Figure 2A), nor was there a correlation between FWLS and PXS score (Supplemental Table 1). These scores fall within the range of moderate-to-severe lung pathology. Fifteen patients had CT pulmonary angiograms performed due to clinical suspicion for PE, of which 5 had evidence of segmental or subsegmental PEs. Of the patients with confirmed PEs, 1 of 5 patients had normal FWLS and underwent CT pulmonary angiography (20%) compared to 4 of 10 patients who had abnormal FWLS and underwent CT pulmonary angiography (40%) (Figure 2B). The 4 patients with abnormal FWLS who underwent CT pulmonary angiography had strain values

Table 4. Echocardiographic Findings Among Intubated COVID-19 Patients.

	All (n = 32)	Normal FWLS (n = 11)	Abnormal FWLS (n = 21)	*P* value
RV FWLS (%), mean ± SD	−17% ± 6%	−24% ± 2%	−14% ± 4%	–
RV basal diameter (cm), mean ± SD	4.22 ± 0.94	4.11 ± 0.83	4.27 ± 1.00	0.670
RV basal diameter > 4.2 cm, n (%)	14 (44%)	5 (45%)	9 (43%)	0.893
TAPSE (cm), mean ± SD	2.25 ± 0.50	2.35 ± 0.49	2.20 ± 0.51	0.426
TAPSE < 1.8 cm, n (%)	5 (15.6%)	0 (%)	5 (24%)	0.083
S' (cm/s), mean ± SD	14.6 ± 3.66	14.4 ± 3.77	14.6 ± 3.70	0.869
RVSP* (mmHg), mean ± SD	30.0 ± 11.5	31.9 ± 13.2	28.9 ± 10.7	0.496
RVSP > 35 mmHg, n (%)	13 (42%)	6 (55%)	7 (33%)	0.260
LA pressure (mmHg)**, mean ± SD	11.6 ± 3.0	11.7 ± 2.4	11.6 ± 3.3	0.893
LA pressure > 14 mmHg, n (%)	4 (13%)	1 (10%)	3 (14%)	0.749
E (cm/s), mean ± SD	76.6 ± 19.9	74.3 ± 21.4	77.6 ± 19.6	0.675
A (cm/s), mean ± SD	76.7 ± 21.1	87.1 ± 16.1	71.4 ± 21.7	0.053
e' (cm/s), mean ± SD	10.7 ± 2.80	10.1 ± 2.39	11.0 ± 2.98	0.379
a' (cm/s), mean ± SD	12.6 ± 3.64	14.6 ± 3.73	11.5 ± 3.21	0.026
LVOT VTI*** (cm), mean ± SD	23.7 ± 5.3	28.1 ± 4.3	21.7 ± 4.3	0.001
LVOT VTI < 18 cm, n (%)	2 (7.1%)	0 (0%)	2 (11%)	0.331

Abbreviations: FWLS, free wall longitudinal strain; RV, right ventricular; SD, standard deviation; TAPSE, tricuspid annular plane systolic excursion; S', peak systolic tricuspid annular velocity; RVSP, right ventricular systolic pressure; LV, left ventricular; LA, left atrium; E, early mitral diastolic filling velocity; A, late mitral diastolic filling velocity; e', early diastolic mitral annular velocity; a', late diastolic mitral annular velocity; LVOT VTI, left ventricular outflow tract velocity time integral.
*Tricuspid regurgitation jet was not visualized in 1 patient. **LA pressure could not be estimated in 1 patient. ***LVOT VTI could not be determined in 4 patients.

that were below the lower (25%) quartile. Examples of scored chest radiographs from patients with normal and abnormal FWLS are shown in Figure 2C.

Discussion

In our cohort of critically ill COVID-19 patients, we found the incidence of pulmonary hypertension (42%) and RV dilation (44%) to be similar to other populations with ARDS[5] and slightly higher than previous reports of RV dysfunction in COVID-19 ranging from 30%-39%.[3,4,14] This is not surprising given that our study included only those with severe illness requiring mechanical ventilation. Abnormal FWLS was present in the majority (66%) of our patients and, unexpectedly, was associated with favorable lung mechanics (i.e. compliance) and lower airway pressures, suggesting that FWLS in this population may not be attributable to alveolar collapse or distension during positive pressure ventilation. Patients with abnormal FWLS did not exhibit worse oxygenation, hypercarbia, or acidosis and, consistent with these findings, did not have radiologic evidence of more severe lung disease to account for the RV impairment. It is possible that prior hypoxemic episodes or sudden changes in transpulmonary pressures, such as during endotracheal intubation, may have contributed to the RV strain patterns detected on echocardiography. Whether strain abnormalities persist after acute changes in RV afterload is an area that warrants further investigation.

Severe COVID-19 illness is not limited to pulmonary manifestations and often involves other organ systems including the brain, liver, and kidneys.[26,27] A possible explanation for our findings, therefore, may be that patients with abnormal FWLS, while not experiencing more severe respiratory illness, may have had more severe multi-organ involvement. However, in the current study, FWLS did not correlate with severity of systemic illness based on clinical risk scores, inflammatory markers, or vasopressor requirements. We consider 2 alternative mechanisms that may explain impaired RV function in our study: 1) pulmonary vascular abnormalities, such as micro or macro thromboembolic phenomena that can increase RV afterload, and 2) direct myocardial injury causing impaired contractility.

Intravascular micro and macro thrombosis has been reported in both non-COVID-19 and COVID-19 ARDS.[28,29] Microthrombosis is much more frequent in COVID-19 ARDS and may contribute to increased total pulmonary vasculature resistance.[11] Enlarged vessels and shunting of blood toward areas of diseased lungs are additional features of COVID-19 infection that may affect RV afterload.[9] A key role of diffuse intravascular thrombosis in RV dysfunction in COVID-19 is supported by the lower platelet counts we observed among patients with abnormal FWLS. A decrease in platelets, while common occurrence in a hyperinflammatory state, is also observed during acute PE due to platelet activation in the pulmonary vasculature.[30,31] Indeed, 4 of the 5 patients diagnosed with PE in our cohort had abnormal strain patterns, although the process by which pulmonary angiography was performed in our patients introduces selection bias. We also expect that pulmonary thrombosis, if leading to abnormal FWLS, would also cause a concomitant rise in pulmonary artery pressures. Pulmonary hypertension was not associated with FWLS in our study, however the accuracy of echocardiography in estimating pulmonary artery pressures is limited at best with a tendency to underestimate.[32,33] A more complete understanding of the role for pulmonary thrombosis in the pathogenesis of RV

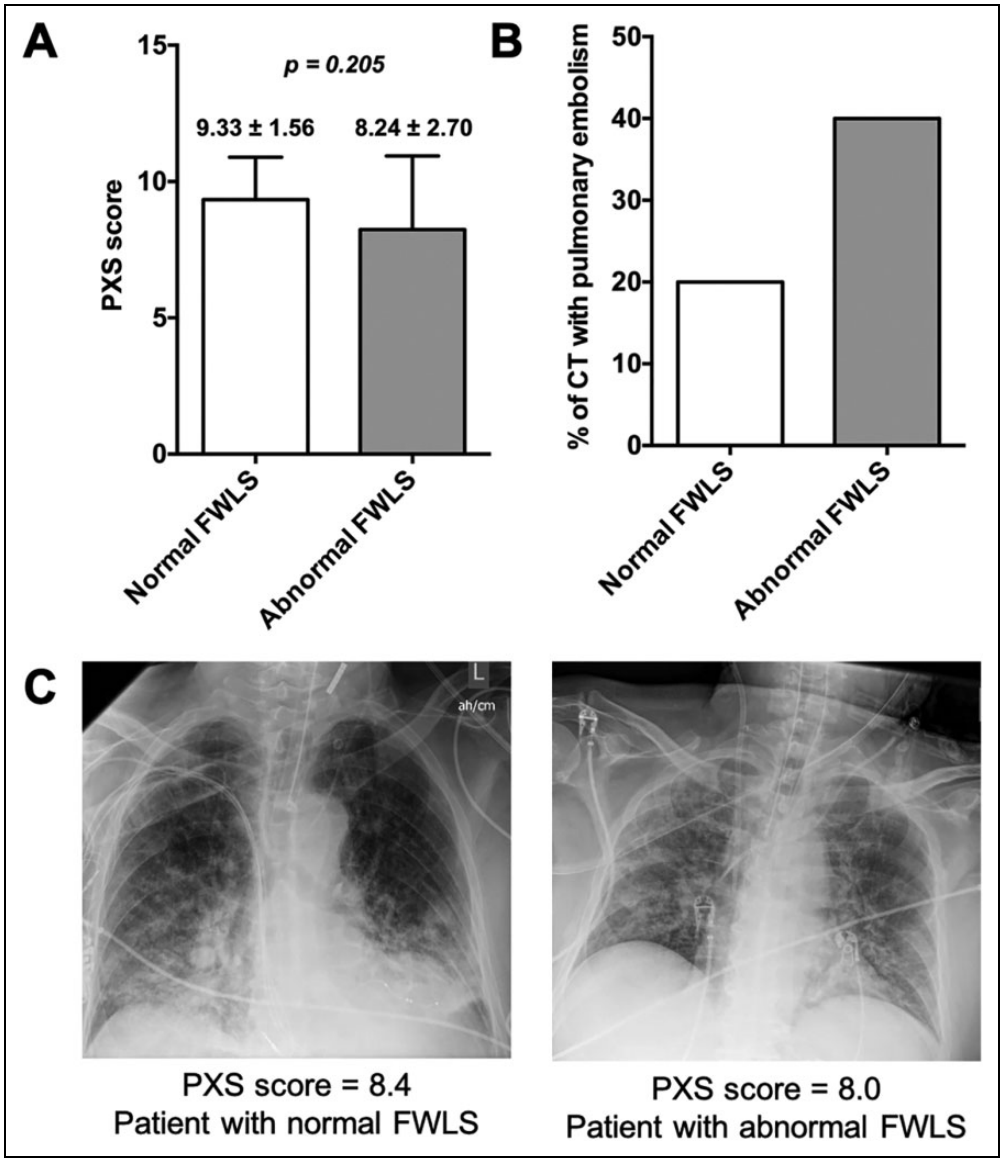

Figure 2. Patients with normal and abnormal right ventricular free wall longitudinal strain (FWLS) had similar COVID-19 lung disease severity scores on chest radiographs (PXS score) and different rates of pulmonary embolism on CT imaging. A) Histogram comparing mean PXS scores $\pm$ standard deviation between patients with normal and abnormal FWLS. B) Patients with abnormal FWLS had a higher rate of pulmonary embolism detected on CT imaging. C) Illustrative examples above from a patient with normal FWLS (left panel) and abnormal FWLS (right panel) show patchy bilateral airspace opacities. The PXS scores of 8.0 and 8.4 reflect moderate radiographic disease severity.

impairment in COVID-19 infection may be gained by direct measurement of pulmonary pressures by catheterization.

Direct myocardial damage may occur in severe COVID-19 either from inflammation or viral entry into cardiomyocytes. Autopsy studies have identified endothelialitis of the pulmonary vasculature as a prominent feature of severe COVID-19 infection.[11,12] Due to its limited contractile reserve, the RV may be particularly susceptible to inflammatory insult. Indeed, macrophage infiltration and interstitial fibrosis have been identified within the myocardium of COVID-19 patients.[34,35] While the virus has proven capable of entry and replication within cardiomyocytes grown *in vitro*, it is unclear whether this occurs in patients.[36] We also considered myocardial ischemia as a possible etiology for RV injury given that many patients in our cohort had elevated high-sensitivity troponin levels. However, we found FWLS to be negatively correlated with troponin levels, i.e. patients with less negative (abnormal) strain values had lower troponin levels, while patients with more negative (normal) strain values had higher troponin levels. This finding argues against direct myocardial injury, either from ischemic insult or myocarditis, as the primary cause of RV dysfunction in our population.

Lastly, we found that abnormal RV FWLS was associated with markers of reduced LV systolic and diastolic function. LV dysfunction in previously normal hearts may be seen during acute pulmonary hypertension as a consequence of ventricular

interdependence.[37] Alternatively, FWLS may provide an early indication of global cardiac impairment in COVID-19 patients, as factors causing direct injury to the RV would also damage the LV. Evaluation of LV strain, while beyond the scope of the current study, may provide better understanding of this relationship.

Limitations

This study has several limitations. First, we report clinical findings on a small, relatively homogenous cohort of mechanically ventilated patients and may be underpowered to detect important differences. The dichotomization of normal and abnormal RV strain could further decrease our ability to detect differences. Second, 15 of our patients were in the prone position at the time of echocardiographic examination. This includes 5 of 11 patients (45%) with normal FWLS and 10 of 21 patients (48%) with abnormal FWLS. While technically feasible,[38] echocardiographic measures have not been validated in this position. Third, we report differences in RV FWLS, which has been shown to provide a more accurate representation of RV function compared to global RV strain, which incorporates septal strain and is likely impacted by LV function.[39] However, the differences between free wall and global strain have not been well characterized among patients with ARDS. Fourth, CT findings were not available for all patients. CT data is reported from a subset of patients for whom the treating clinicians had suspicion for PE and should be interpreted with caution given selection bias. Lastly, the lack of a comparator group of non-COVID-19 patients with ARDS on which to compare our findings is an important limitation that should be addressed in a future study.

Conclusion

Our findings suggest the need for alternative explanations for RV dysfunction in severe COVID-19 illness beyond positive pressure ventilation, poor lung compliance, and alveolar damage. FWLS may be associated with intravascular micro and macro thrombosis in COVID-19 infection that does not appear to be related to abnormal lung mechanics or ventilatory pressures. Further work is required for a more thorough understanding of the mechanism for the development of RV dysfunction and its prognostic implications in this population.

Abbreviations

APACHE, acute physiologic assessment and chronic health evaluation; ARDS, acute respiratory distress syndrome; BMI, body mass index; CRP, C-reactive protein; CKD, chronic kidney disease; COVID-19, coronavirus disease 2019; CK, creatinine kinase; CT, computed tomography; FWLS, free wall longitudinal strain; HTN, hypertension; IQR, interquartile range; LA, left atrium; LDH, lactate dehydrogenase; LV, left ventricular; LVOT VTI, left ventricular outflow tract velocity time integral; *P*, pressure; PE, pulmonary embolism; PEEP, positive end expiratory pressure; PXS, pulmonary x-ray severity score; RV, right ventricular; RVSP, right ventricular systolic pressure; SD, standard deviation; SOFA, sequential organ failure assessment; TAPSE, tricuspid annular plane systolic excursion; TV, tidal volume; VIS, vasoactive inotropic score.

Authors' Note

Principal Investigators for the Nitric Oxide Study include Lorenzo Berra, MD (Massachusetts General Hospital), Louie K. Scott, MD (Louisiana State University), Pankaj Arora, MD (University of Alabama at Birmingham), and Somnath Bose, MD (Beth Israel Deaconess Medical Center). LEG made substantial contributions to the conception and design of the work, performed and analyzed all echocardiograms, performed statistical analyses, and drafted the manuscript. RDF made substantial contributions to the acquisition of data, statistical analyses, and revising of the work. ML, MDL, JKC, and BPL made substantial contributions to the analysis and interpretation of chest imaging data and revising of the work. MIC made substantial contributions to the acquisition of data and revising of the work. PA made substantial contributions to the analysis and interpretation of echocardiographic data and revising of the work. ALM made substantial contributions to the acquisition of data and revising of the work. FI, EAB, and LB made substantial contributions to the analysis and interpretation of data and revising of the work. MGC oversaw all aspects of the work including substantial contributions to the conception and design, analyzed all echocardiograms, interpreted the data, and revised the manuscript. All authors approve of the final submitted manuscript and agree to be accountable for the accuracy and integrity of the work. This study was approved by the Mass General Brigham Institutional Review Board (2020P000787). Informed consent was obtained from each patient or their surrogate prior to enrollment.

Declaration of Conflicting Interests

The author(s) declared the following potential conflicts of interest with respect to the research, authorship, and/or publication of this article: LB receives salary support from K23 HL128882/NHLBI NIH as principal investigator for his work on hemolysis and nitric oxide. LB receives technologies and devices from iNO Therapeutics LLC, Praxair Inc., Masimo Corp. LB receives funding from a Fast Grant for COVID-19 research at Mercatus Center of George Mason University and from iNO Therapeutics LLC. BPL is a textbook associate editor and author for Elsevier, Inc. and receives royalties. JKC reports grants from GE Healthcare, non-financial support from AWS, and grants from Genentech Foundation outside of the submitted work.

Funding

The author(s) disclosed receipt of the following financial support for the research, authorship, and/or publication of this article: This study was supported in part by the Reginald Jenney Endowment Chair at Harvard Medical School, by Sundry Funds at Massachusetts General Hospital, by laboratory funds of the Anesthesia Center for Critical Care Research of the Department of Anesthesia, Critical Care and Pain Medicine at Massachusetts General Hospital, by a Fast Grant for COVID-19 research at Mercatus Center of George Mason University, and by a grant from iNO Therapeutics LLC. This research was carried out in part at the Athinoula A. Martinos Center for Biomedical Imaging at the Massachusetts General Hospital, using resources provided by the Center for Functional Neuroimaging Technologies, P41EB015896, a P41 Biotechnology Resource Grant supported by the National Institute of Biomedical Imaging and Bioengineering (NIBIB), National Institutes of Health. GPU computing resources were provided by the Massachusetts General Hospital and Brigham and Women's Hospital Center for Clinical Data Science.

ORCID iD

Lauren E. Gibson, MD https://orcid.org/0000-0003-4549-1678

Supplemental Material

Supplemental material for this article is available online.

References

1. Shi S, Qin M, Shen B, et al. Association of cardiac injury with mortality in hospitalized patients with COVID-19 in Wuhan, China. *JAMA Cardiol*. 2020;5(7):802-810. doi:10.1001/jamacardio.2020.0950
2. Deng Q, Hu B, Zhang Y, et al. Suspected myocardial injury in patients with COVID-19: evidence from front-line clinical observation in Wuhan, China. *Int J Cardiol*. 2020;311:116-121. doi:10.1016/j.ijcard.2020.03.087
3. Argulian E, Sud K, Vogel B, et al. Right ventricular dilation in hospitalized patients with COVID-19 infection. *JACC Cardiovasc Imaging*. 2020;13(11):2459-2461. doi:10.1016/j.jcmg.2020.05.010
4. Szekely Y, Lichter Y, Taieb P, et al. Spectrum of cardiac manifestations in COVID-19. *Circulation*. 2020;142(4):342-353. doi:10.1161/CIRCULATIONAHA.120.047971
5. Zochios V, Parhar K, Tunnicliffe W, Roscoe A, Gao F. The right ventricle in ARDS. *Chest*. 2017;152(1):181-193. doi:10.1016/j.chest.2017.02.019
6. Whittenberger JL, Mcgregor M, Berglund E, Borst HG. Influence of state of inflation of the lung on pulmonary vascular resistance. *J Appl Physiol*. 1960;15:878-882. doi:10.1152/jappl.1960.15.5.878
7. Zapol WM, Snider MT. Pulmonary hypertension in severe acute respiratory failure. *N Engl J Med*. 1977;296(9):476-480. doi:10.1056/NEJM197703032960903
8. Greene R, Lind S, Jantsch H, et al. Pulmonary vascular obstruction in severe ARDS: angiographic alterations after I.V. fibrinolytic therapy. *AJR Am J Roentgenol*. 1987;148(3):501-508. doi:10.2214/ajr.148.3.501
9. Lang M, Som A, Mendoza DP, et al. Hypoxaemia related to COVID-19: vascular and perfusion abnormalities on dual-energy CT. *Lancet Infect Dis*. 2020;20(12):1365-1366. doi:10.1016/S1473-3099(20)30367-4
10. Lang M, Som A, Carey D, et al. Pulmonary vascular manifestations of COVID-19 pneumonia. *Radiol Cardiothorac Imaging*. 2020;2(3):e200277. doi:10.1148/ryct.2020200277
11. Ackermann M, Verleden SE, Kuehnel M, et al. Pulmonary vascular endothelialitis, thrombosis, and angiogenesis in Covid-19. *N Engl J Med*. 2020;383(2):120-128. doi:10.1056/NEJMoa2015432
12. Varga Z, Flammer AJ, Steiger P, et al. Endothelial cell infection and endotheliitis in COVID-19. *Lancet*. 2020;395(10234):1417-1418. doi:10.1016/S0140-6736(20)30937-5
13. Lee J-H, Park J-H. Strain analysis of the right ventricle using two-dimensional echocardiography. *J Cardiovasc Imaging*. 2018;26(3):111-124. doi:10.4250/jcvi.2018.26.e11
14. Li Y, Li H, Zhu S, et al. Prognostic value of right ventricular longitudinal strain in patients with COVID-19. *JACC Cardiovasc Imaging*. 2020;13(11):2287-2299. doi:10.1016/j.jcmg.2020.04.014
15. Lei C, Su B, Dong H, et al. Protocol of a randomized controlled trial testing inhaled nitric oxide in mechanically ventilated patients with severe acute respiratory syndrome in COVID-19 (SARS-CoV-2). *medRxiv*. 2020. doi:10.1101/2020.03.09.20033530
16. Knaus WA, Draper EA, Wagner DP, Zimmerman JE. APACHE II: a severity of disease classification system. *Crit Care Med*. 1985;13(10):818-829.
17. Vincent J-L, Moreno R, Takala J, et al. The SOFA (Sepsis-related Organ Failure Assessment) score to describe organ dysfunction/failure: On behalf of the Working Group on Sepsis-Related Problems of the European Society of Intensive Care Medicine (see contributors to the project in the appendix). *Intensive Care Med*. 1996;22(7):707-710. doi:10.1007/BF01709751
18. Kara İ, Sargin M, Bayraktar YŞ, Eyiol H, Duman I, Çelik JB. The use of Vasoactive-Inotropic Score in Adult Patients with Septic Shock in Intensive Care. *Yoğun Bakım Derg*. 2019;10(1):23-30. doi:10.33381/DCBYBD.2019.2057
19. Rudski LG, Lai WW, Afilalo J, et al. Guidelines for the echocardiographic assessment of the right heart in adults: a report from the American Society of Echocardiography endorsed by the European Association of Echocardiography, a registered branch of the European Society of Cardiology, and the Canadian Society of Echocardiography. *J Am Soc Echocardiogr*. 2010;23(7):685-713; quiz 786-788. doi:10.1016/j.echo.2010.05.010
20. Forfia PR, Fisher MR, Mathai SC, et al. Tricuspid annular displacement predicts survival in pulmonary hypertension. *Am J Respir Crit Care Med*. 2006;174(9):1034-1041. doi:10.1164/rccm.200604-547OC
21. Park J-H, Marwick TH. Use and Limitations of E/e' to assess left ventricular filling pressure by echocardiography. *J Cardiovasc Ultrasound*. 2011;19(4):169-173. doi:10.4250/jcu.2011.19.4.169
22. Badano LP, Kolias TJ, Muraru D, et al. Standardization of left atrial, right ventricular, and right atrial deformation imaging using two-dimensional speckle tracking echocardiography: a consensus document of the EACVI/ASE/Industry Task Force to standardize deformation imaging. *Eur Heart J Cardiovasc Imaging*. 2018;19(6):591-600. doi:10.1093/ehjci/jey042
23. Lang RM, Badano LP, Mor-Avi V, et al. Recommendations for cardiac chamber quantification by echocardiography in adults: an update from the American Society of Echocardiography and the European Association of Cardiovascular Imaging. *J Am Soc Echocardiogr Off Publ Am Soc Echocardiogr*. 2015;28(1):1-39.e14. doi:10.1016/j.echo.2014.10.003
24. Li MD, Arun NT, Gidwani M, et al. Automated assessment and tracking of COVID-19 pulmonary disease severity on chest radiographs using convolutional siamese neural networks. *Radiol Artif Intell*. 2020;2(4):e200079. doi:10.1148/ryai.2020200079
25. Li MD, Arun NT, Aggarwal M, et al. Improvement and multipopulation generalizability of a deep learning-based chest radiograph severity score for COVID-19. *medRxiv*. 2020. doi:10.1101/2020.09.15.20195453
26. Puelles VG, Lütgehetmann M, Lindenmeyer MT, et al. Multiorgan and renal tropism of SARS-CoV-2. *N Engl J Med*. 2020;383(6):590-592. doi:10.1056/NEJMc2011400
27. White-Dzuro G, Gibson LE, Zazzeron L, et al. Multisystem effects of COVID-19: a concise review for practitioners.

Postgrad Med. 2020;133(1):20-27. doi:10.1080/00325481.2020.1823094

28. Dolhnikoff M, Duarte-Neto AN, de Almeida Monteiro RA, et al. Pathological evidence of pulmonary thrombotic phenomena in severe COVID-19. *J Thromb Haemost*. 2020;18(6):1517-1519. doi:10.1111/jth.14844
29. Lai PS, Mita C, Thompson BT. What is the clinical significance of pulmonary hypertension in acute respiratory distress syndrome? A review. *Minerva Anestesiol*. 2014;80(5):574-585.
30. Monreal M, Lafoz E, Casals A, Ruíz J, Arias A. Platelet count and venous thromboembolism. A useful test for suspected pulmonary embolism. *Chest*. 1991;100(6):1493-1496. doi:10.1378/chest.100.6.1493
31. Chung T, Connor D, Joseph J, et al. Platelet activation in acute pulmonary embolism. *J Thromb Haemost*. 2007;5(5):918-924. doi:10.1111/j.1538-7836.2007.02461.x
32. Fisher MR, Forfia PR, Chamera E, et al. Accuracy of Doppler echocardiography in the hemodynamic assessment of pulmonary hypertension. *Am J Respir Crit Care Med*. 2009;179(7):615-621. doi:10.1164/rccm.200811-1691OC
33. Rich JD, Shah SJ, Swamy RS, Kamp A, Rich S. Inaccuracy of Doppler echocardiographic estimates of pulmonary artery pressures in patients with pulmonary hypertension: implications for clinical practice. *Chest*. 2011;139(5):988-993. doi:10.1378/chest.10-1269
34. Oudit GY, Kassiri Z, Jiang C, et al. SARS-coronavirus modulation of myocardial ACE2 expression and inflammation in patients with SARS. *Eur J Clin Invest*. 2009;39(7):618-625. doi:10.1111/j.1365-2362.2009.02153.x
35. Lindner D, Fitzek A, Bräuninger H, et al. Association of cardiac infection with SARS-CoV-2 in confirmed COVID-19 autopsy cases. *JAMA Cardiol*. 2020;5(11):1281-1285. doi:10.1001/jamacardio.2020.3551
36. Sharma A, Garcia G, Arumugaswami V, Svendsen CN. Human iPSC-Derived Cardiomyocytes are Susceptible to SARS-CoV-2 Infection. *bioRxiv*. 2020;1(4):100052. doi:10.1101/2020.04.21.051912
37. Amà R, Leather HA, Segers P, Vandermeersch E, Wouters PF. Acute pulmonary hypertension causes depression of left ventricular contractility and relaxation. *Eur J Anaesthesiol*. 2006;23(10):824-831. doi:10.1017/S0265021506000317
38. Gibson LE, Di Fenza R, Berra L, Bittner EA, Chang MG. Transthoracic echocardiography in prone patients with acute respiratory distress syndrome: a feasibility study. *Crit Care Explor*. 2020;2(8):e0179. doi:10.1097/CCE.0000000000000179
39. Focardi M, Cameli M, Carbone SF, et al. Traditional and innovative echocardiographic parameters for the analysis of right ventricular performance in comparison with cardiac magnetic resonance. *Eur Heart J Cardiovasc Imaging*. 2015;16(1):47-52. doi:10.1093/ehjci/jeu156